The electronic spectrum of the SiC radical: A theoretical study

ARTICLE *in* JOURNAL OF MOLECULAR SPECTROSCOPY · JULY 2007

Impact Factor: 1.48 · DOI: 10.1016/j.jms.2007.05.007

2 AUTHORS, INCLUDING:

Anup Pramanik
Visva Bharati University
27 PUBLICATIONS **99** CITATIONS

SEE PROFILE

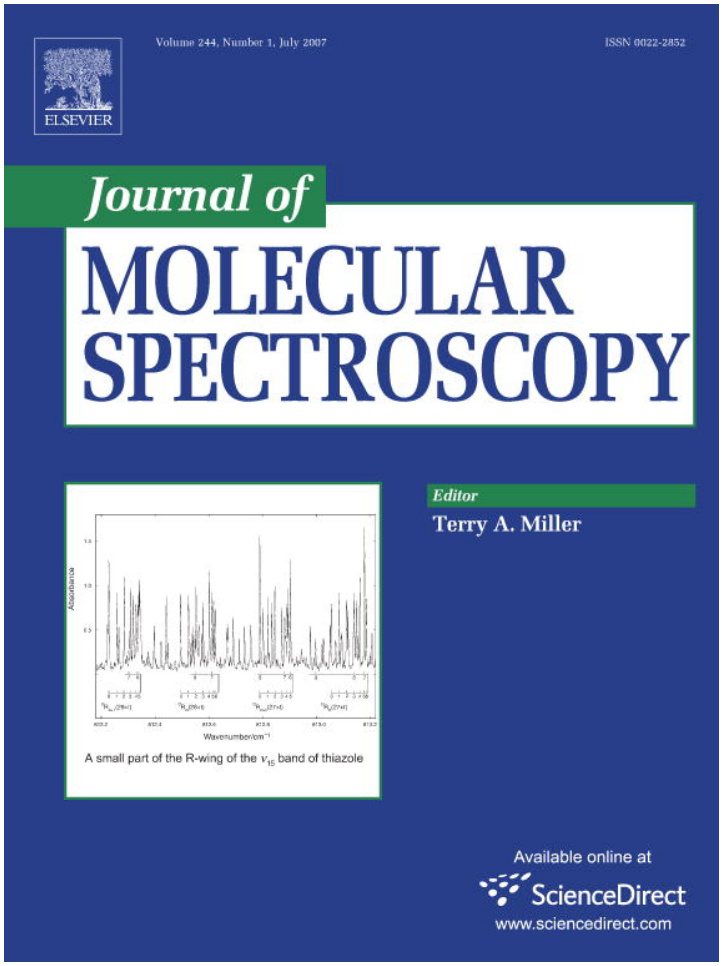

Available online at www.sciencedirect.com
ScienceDirect
Journal of Molecular Spectroscopy 244 (2007) 13–23
Journal of MOLECULAR SPECTROSCOPY
www.elsevier.com/locate/jms

The electronic spectrum of the SiC radical: A theoretical study

Anup Pramanik, Kalyan Kumar Das *

Department of Chemistry, Physical Chemistry Section, Jadavpur University, Kolkata 700 032, India

Received 27 April 2007
Available online 2 June 2007

Abstract

Electronic structure and spectroscopic properties of the low-lying electronic states of the SiC radical have been determined from the ab initio based configuration interaction calculations. Potential energy curves of 32 Λ–S states of singlet, triplet, and quintet spin multiplicities have been constructed. Spectroscopic constants (r_e, T_e, and ω_e) of 23 states within 6 eV are reported and compared with the existing data. The dipole moments (μ_e) of most of these states at their respective equilibrium bond lengths have been computed. Effects of the spin–orbit coupling on the spectroscopic properties of SiC have been studied. The $E^3\Pi$ state is found to be an important one which has not been studied before. A transition of the type $E^3\Pi$–$X^3\Pi$ is predicted to take place in the range 25 000–26 000 cm^{-1}. The partial radiative lifetimes for several electric dipole allowed transitions such as $A^3\Sigma^+$–$X^3\Pi$, $B^3\Sigma^+$–$X^3\Pi$, $C^3\Pi$–$X^3\Pi$, $D^3\Delta$-$X^3\Pi$, $E^3\Pi$–$X^3\Pi$ etc. have been reported.

Keywords: Silicon carbide; Configuration interaction; Electronic spectrum; Spectroscopic constants; Potential energy curves

1. Introduction

The simple diatomic SiC radical is known to be an important component of the carbon star. It is also present in interstellar regions of space [1]. Though astrophysically important, the spectroscopy of this radical was not observed in laboratory for a long time. The major difficulty to study the silicon–carbon compounds was that it needed a very high temperature to vaporize these elements. Bondybey [2] and Michalopoulos et al. [3] attempted experiments using laser vaporization of silicon carbide rod. But the detection of the SiC radical was unsuccessful. Although Si_2 and C_2 are spectroscopically well known species, the spectroscopic identification of SiC has been made much later. However, ab initio calculations of SiC are performed before the experimental detection. Lutz and Ryan [4] have performed the configuration interaction (CI) calculations and found that the ground state of the mixed first row–second row diatomic is $^3\Pi$. Bruna et al. [5] have also carried out large scale CI calculations for the potential curves of the isovalent series of diatomic species, CN^+, Si_2, SiC, CP^+, and SiN^+ in their low-lying states. The results of these calculations for the SiC radical have agreed well with those of the previous calculations [4]. Rohlfing and Martin [6] have studied the structure and spectroscopic properties of the isovalent diatomic molecules such as C_2, Si_2, and SiC. These authors have used Moller–Plesset perturbation theory based on UHF reference function as well as externally contracted CI based on a multireference function of the complete-active-space type for determining the spectroscopic constants of a few low-lying states. Meanwhile, low-lying electronic states of SiC^- and electron affinity of SiC have been studied by Anglada et al. [7] from large scale CI calculations. Dohman et al. [8] have made a comparison among various isoelectronic radicals possessing eight valence electrons. The CASSCF and contracted CI calculations have been performed by Larsson [9] to study the potential curves of $X^3\Pi$, $B^3\Sigma^+$, and $C^3\Pi$ states of the SiC molecule. The author has predicted transitions between the ground state and the B and C states to occur in the wave length range 4000–6000 Å. Bauschlicher and Langhoff [10] have performed CI calculations at various levels of electron correlation to compute the spectroscopic

* Corresponding author.
E-mail address: kkdas@chemistry.jdvu.ac.in (K.K. Das).

0022-2852/$ - see front matter © 2007 Elsevier Inc. All rights reserved.
doi:10.1016/j.jms.2007.05.007

constants of $X^3\Pi$ and $A^3\Sigma^-$ states of SiC. Their best estimates of r_e, ω_e, and D_e for the ground state of the radical were 1.719 Å, 962 cm^{-1}, and 4.4 eV, respectively.

The SiC radical was first observed [11] by high-resolution Fourier transform emission spectroscopy from a composite wall hollow cathode. The 0–0 band of the $d^1\Sigma^+$–$b^1\Pi$ system of SiC has been observed near 6100 cm^{-1}. This has been confirmed by ab initio calculations performed at different level of accuracy. Molecular constants of several low-lying states, namely $X^3\Pi$, $A^3\Sigma^-$, $a^1\Sigma^+$, $b^1\Pi$, $c^1\Delta$, and $d^1\Sigma^+$ of SiC are predicted from these calculations. The results are found to be comparable with the predictions of Bauschlicher and Langhoff [10]. The ground state of SiC has been characterized from the microwave transition observed by Cernicharo et al. [12]. The $A^3\Sigma^-$–$X^3\Pi$ system of SiC is analogous to the Ballik–Ramsay system of C_2. Brazier et al. [13] have observed the 0–0 band of this system in emission near 4500 cm^{-1} and the reported bond lengths are 1.81356 and 1.72187 Å for $A^3\Sigma^-$ and $X^3\Pi$ states, respectively. The A–X band was found to be weak because of the difficulty in making the SiC radical. Multireference CI calculations have been performed by Langhoff and Bauschlicher [14] to study the $A^3\Sigma^-$–$X^3\Pi$ infrared transition in the radical. The 0–0 band of the A–X transition has also been reassigned in another theoretical study [15]. The dipole moment functions of $A^3\Sigma^-$ and $X^3\Pi$, and the transition moment functions as well as radiative lifetimes of the A–X transition have also been reported. Martin et al. [16] have computed three lowest states, $X^3\Pi$, $A^3\Sigma^-$, and $a^1\Sigma^+$ of SiC using augmented coupled cluster methods and different basis sets. Thermochemistry of the radical has also been reported by these authors. Butenhoff and Rohlfing [17] have studied the $C^3\Pi$–$X^3\Pi$ band system of the jet-cooled SiC radical using a laser induced fluorescence (LIF) spectroscopy. The vibrational energies and rotational constants for the lowest few vibrational levels of both $C^3\Pi$ and $X^3\Pi$ states of SiC have been determined by these authors. Almost at the same time, Ebben et al. [18] have measured seven rovibronic bands belonging to the $C^3\Pi$–$X^3\Pi$ transition in SiC produced by the laser vaporization in combination with supersonic cooling. The radiative lifetimes of the $C^3\Pi$ state were found to vary from 2886 to 499 ns in the lowest seven vibrational levels. Singles and doubles CI calculations from single SCF configuration have been carried out by McLean et al. [19] on a series of diatomic species including SiC and SiC^-. Some spectroscopic information of $X^3\Pi$, $A^3\Sigma^-$, $b^1\Pi$, and $c^1\Delta$ states of SiC and the $^2\Pi$ state of SiC^- have been reported. The millimeter-wave rotational spectra with hyperfine structure of two stable isotopes with nuclear spin, namely ^{29}SiC and Si^{13}C, were detected in the ground state [20,21]. The vibrational and adiabatic ionization energies and electron affinities of Si_nC and Si_nO ($n = 1$–3) molecules have been reported by Boldyrev et al. [22] from large-scale ab initio calculations at different levels of correlation.

Grutter et al. [23] have identified the electronic absorption spectra of SiC^- and SiC in 5 K neon matrices using mass-selected deposition. The neutralization of the anion leads to the observation of a new band system $B^3\Sigma^+ \leftarrow X^3\Pi$ of SiC in addition to the known systems, namely $A^3\Sigma^- \leftarrow X^3\Pi$ and $C^3\Pi \leftarrow X^3\Pi$. The B–X band has the origin at 11 749 cm^{-1}, while the ω_e value for the $B^3\Sigma^+$ state of SiC in neon matrix has been reported to be 1178 cm^{-1}. However, no gas phase data is available for this state. Recently [24], the infrared emission spectrum of the $A^3\Sigma^-$–$X^3\Pi$ electronic transition of the SiC radical in the gas phase has been observed using a high resolution Fourier transform spectrometer. Three bands, 0–1, 0–0, and 1–0 of this system are found in 2770, 3723, and 4578 cm^{-1}, respectively.

In this paper, we have performed ab initio based multireference singles and doubles CI (MRDCI) calculations to study the electronic structure and spectroscopic properties of the SiC radical in low-lying singlet, triplet, and quintet states. The effects of the spin-coupling on the spectroscopic properties of these states have been studied. Potential energy curves of the low-lying states of SiC have been constructed with and without spin–orbit coupling. The radiative lifetimes of some of the excited states have been predicted and compared with the available data.

2. Method of computations

The average relativistic effective potentials (AREP) of Pacios and Christiansen [25] are used to replace the $1s^22s^22p^6$ core electrons of the Si atom and $3s^23p^2$ valence electrons are kept available for the CI calculations. For the carbon atom, the AREP of the same authors have been employed. The total number of active electrons in the CI space is, therefore eight. The 4s4p Gaussian basis sets of Pacios and Christiansen [25] for Si are augmented with some diffuse and polarization functions. Three s functions ($\xi_s = 0.04525$, 0.02715, and $0.0163a_0^{-2}$), two p functions ($\xi_p = 0.06911$ and $0.02499a_0^{-2}$), five d functions ($\xi_d = 4.04168$, 1.46155, 0.52852, 0.19112, and $0.06911a_0^{-2}$), and two f functions ($\xi_f = 0.19112$ and $0.06911a_0^{-2}$) are added [26]. The first two sets of d functions are contracted using coefficients of 0.054268 and 0.06973. Similarly, the two f functions are contracted using the coefficients of 0.29301 and 0.536102. The final basis set for Si used in the present CI calculations is (7s6p5d2f/7s6p4d1f). For the carbon atom, the (4s4p) basis set of Pacios and Christiansen [25] has been enhanced by adding two sets of d functions of exponents 1.2 and 0.35.

At each internuclear distance of SiC, we have performed self-consistent-field (SCF) calculations for the $(\sigma^2\sigma^2\pi^2)$ $^3\Sigma^-$ state using the above mentioned basis sets. The entire calculations are carried out in the C_{2v} subgroup keeping Si at the origin and C in the $+z$ axis. The symmetry adapted SCF-MOs are subsequently used for the generation of configurations in the CI calculations. Throughout the calculations we have employed the MRDCI methodology of Buenker and coworkers [27–33] which uses perturbative correction and energy extrapolation techniques. The

table-CI algorithm is used to handle open shell configurations which appear due to the excitation process. For each of the four irreducible representations of C_{2v} with a given spin multiplicity, we have chosen a set of reference configurations. All possible single and double excitations are carried out from these reference configurations. A maximum of eight roots for singlets and triplets, and four roots for quintets are optimized. The total number of generated configurations easily exceeds several million. However, the size of the CI space is reduced to a large extent by using the configuration selection techniques. We have used a configuration selection-threshold of 10^{-6} hartree so that the number of selected configurations remains within 200 000. The table direct CI version [34] of the MRDCI code has been used throughout the calculation. The sums of squares of the coefficients of the reference configurations for each root remain around 0.9. The energy extrapolation method has been used to estimate energies at zero threshold. The higher excitations are taken into account by the multireference analogue of the Davidson's correction [35,36] which has led to the estimation of full-CI energies.

The spin–orbit interaction is included in the calculation by two-step variational calculations. We have allowed all the spin components of low-lying Λ–S states of SiC to interact. The spin–orbit operators, which are compatible with the AREPs of both the atoms of SiC, are taken from Pacios and Christiansen [25]. The diagonals of the spin-included Hamiltonian matrix consist of estimated full-CI energies of the Λ–S CI calculations. The off-diagonal elements are computed using the spin-orbit operators and Λ–S CI wave functions. The Wigner–Eckart theorem and spin-projection techniques are employed for this purpose. The sizes of the secular equations of A_1, A_2, and B_1/B_2 blocks in the C_{2v}^2 double group are 41×41, 41×41, and 40×40, respectively, for some selected number of roots of Λ–S symmetries of the molecule. The details of the spin–orbit CI treatment are discussed elsewhere [37].

Spectroscopic constants of low-lying Λ–S and Ω states of SiC are calculated by fitting their potential energy curves. The vibrational energies and wave functions are then obtained by solving one-dimensional nuclear Schrödinger equations numerically. These are used for the calculation of transition dipole moments for the pair of vibrational functions in a particular transition. In the subsequent calculations, Einstein spontaneous emission coefficients and transition probabilities are computed. Radiative lifetimes of some of the excited states of SiC are estimated from these data.

3. Results and discussion

3.1. Spectroscopic constants and potential energy curves of Λ–S states

The ground states of both C and Si atoms are in the ^3P_g symmetry. The combination of these states generates as many as 18 Λ–S states of singlets, triplets, and quintet spin multiplicities. Therefore, the lowest dissociation limit, $Si(^3P_g)+C(^3P_g)$ of SiC correlates with $\Sigma^+(2)$, Σ^-, $\Pi(2)$, and Δ states. The second dissociation limit, $Si(^1D_g)+C(^3P_g)$ correlates with triplets, namely $^3\Sigma^+$, $^3\Sigma^-(2)$, $^3\Pi(3)$, $^3\Delta(2)$, and $^3\Phi$. The relative energy of this limit computed from the CI calculation of the SiC molecule at a very large bond distance is about 7000 cm^{-1} which is 800–900 cm^{-1} higher than the *J*-averaged observed value [38]. The next two dissociation limits also correlate only with the excited triplets of SiC. The combination of $Si(^1D_g)$ and $C(^1D_g)$ generates a set of 15 excited singlet states of SiC. The relative energy of these states at the dissociation limit is about 16 500 cm^{-1}.

Potential energy curves of singlet, triplet, and quintet states of SiC without spin–orbit coupling are shown in Figs. 1a–c. All the states correlating with the lowest dissociation limit and a few excited states dissociating into higher asymptotes are studied here. The computed spectroscopic constants (r_e, ω_e, T_e) of 23 Λ–S states are tabulated in Table 1. The computed bond length of the SiC radical in the ground state ($X^3\Pi$) is 1.74 Å which is nearly 0.02 Å longer than the observed data. The ground-state bond length obtained in earlier calculations at various level of theories varies between 1.721 and 1.75 Å. The vibrational frequency (ω_e) of the ground state obtained in the present calculation is 930 cm^{-1} which is about 35 cm^{-1} smaller than the observed value. A comparison of the present data with other theoretical results is shown in Table 1. The ground state of the SiC radical is dominated by the $\sigma_1^2\sigma_2\pi_1^3(80\%)$ configuration at r_e. The σ_1 MO is mainly a bonding combination of s and p_z orbitals of Si and C atoms, while σ_2 has the antibonding character and is mostly localized on the silicon atom. The π_1 MO is a strongly bonding, comprising the $p_{x/y}$ orbitals of the two atoms. The ground-state dissociation energy (D_e) of SiC computed here is 4.05 eV, which is somewhat lower than the thermochemical D_0^0 value of 4.64 eV [39,40]. The MRD-CI calculations [41] with DZP+bond functions have reported a D_e value of 4.3 eV.

The $A^3\Sigma^-$ state is the first excited state of SiC. Its computed transition energy (T_e) is 3985 cm^{-1} which compares well with the experimental or other theoretical data shown in Table 1. The observed 0–0 band of the $A^3\Sigma^-$–$^3X\Pi$ system has been found near 4500 cm^{-1} from which a T_{00} value of 4578 cm^{-1} is obtained [13]. However, Langhoff and Bauschlicher [14] suggested an alternative assignment of the band to a 1–0 transition. These authors have established the 0–0 band at $3700 + 200$ cm^{-1} from the theoretical calculations using atomic natural orbitals. The equilibrium bond length of the $A^3\Sigma^-$ state estimated here is about 1.82 Å which agrees well with the available values as listed in Table 1. The ω_e value of this state, obtained in the present calculations, is 857 cm^{-1} which is very close to the values found in other calculations [14,15]. Around the potential minimum, the $A^3\Sigma^-$ state is dominated by the $\sigma_1^2\sigma_2^2\pi_1^2(88\%)$ configuration in which the π_1 MO has a similar bonding characteristic as in the ground state.

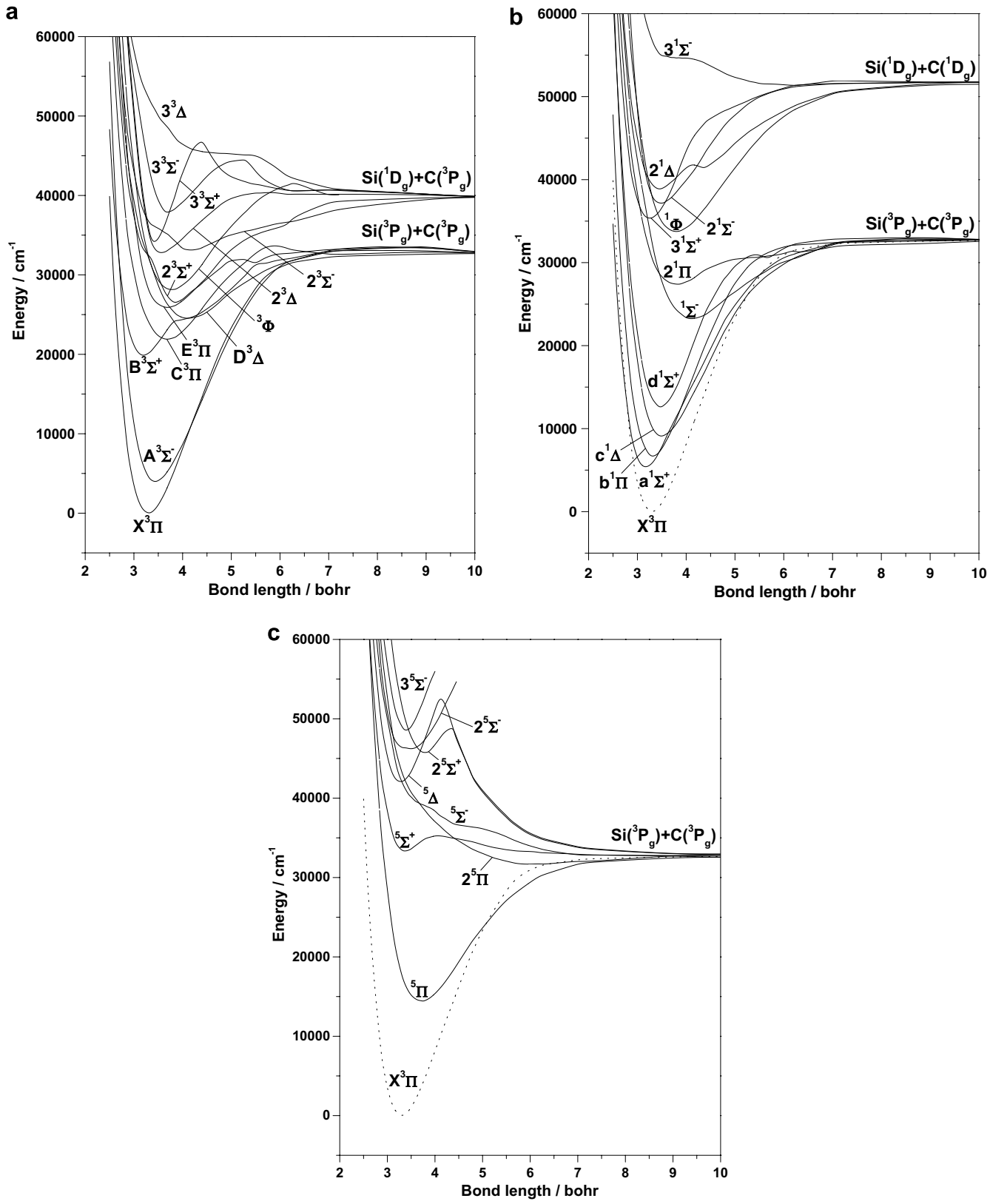

Fig. 1. Computed potential energy curves of low-lying Λ–S states of the SiC radical: (a) singlets, (b) triplets, and (c) quintets.

The lowest singlet state of SiC is $a^1\Sigma^+$ which originates from the $\sigma_2 \rightarrow \pi_1$ transition. The dominant closed shell configuration describing the state is $\sigma_1^2\pi_1^4(70\%)$. The state is very strongly bound with a binding energy of about 3.33 eV. Its estimated transition energy is 5325 cm^{-1} with an equilibrium bond length of 1.68 Å which is shorter than

Table 1
Spectroscopic constants of low-lying states of SiC

State	T_e/cm^{-1}		r_e/Å		ω_e/cm^{-1}		μ_e/D
	Expt.	Calc.	Expt.	Calc.	Expt.	Calc.	
$X^3\Pi$		0	[1.72187][a]	1.74	[965.16][c]	930	1.62
			[1.7182][c]	(1.721)[b]		(957)[b]	
				(1.732)[h]		(954.2)[h]	
				(1.722)[i]		(927)[i]	
				(1.724)[j]		(978.7)[j]	
$A^3\Sigma^-$	[4500][a]	3985	[1.81356][a]	1.82		857	2.55
	[3773.31][g]	(3700 ± 200)[b]	[1.802][g,i]	(1.788)[e]		(862)[f]	
		(3619)[i]		(1.82)[b]		(865)[b]	
		(3831)[j]				(855)[j]	
$a^1\Sigma^+$		5325		1.68		975	2.14
		(5079)[i]		(1.677)[i]		(955)[i]	
		(4355)[j]				(1053)[j]	
$b^1\Pi$		6725		1.75		930	1.81
		(7259)[i]		(1.713)[e]		(963)[i]	
$c^1\Delta$		9135		1.85		790	2.31
		(9094)[i]		(1.81)[e]		(855)[k]	
		(9306)[j]					
$d^1\Sigma^+$		12 705		1.84		880	2.25
		(12338)[i]		(1.794)[i]		(980)[j]	
		(11614)[j]					
$^5\Pi$		14460		1.97		635	0.97
$B^3\Sigma^+$		19800		1.68		890	1.89
		(18954)[h]		(1.669)[h]		(913)[h]	
$C^3\Pi$	[22830.4][c]	21 915	[1.919][c]	1.95	[615.7][c]	580	0.91
	[22829.46][d]	(22768)[h]		(1.908)[h]	[618.85][d]	(615.8)[h]	
$^1\Sigma^-$		23245		2.18		490	0.97
$D^3\Delta$		24485		2.18		508	0.94
$E^3\Pi$		25875		1.94		600	1.32
$2^1\Pi$		27415		2.02		480	1.17
$^3\Phi$		28465		2.02		570	0.93
$^5\Sigma^+$		33355		1.78		745	0.95
$^1\Phi$		33750		2.01		585	1.05
$3^1\Sigma^+$		35125		1.72		920	1.09
$2^1\Sigma^-$		37175		1.84		800	1.42
$2^1\Delta$		38940		1.82		710	1.55
$^5\Delta$		42005		1.73		963	1.36
$2^5\Sigma^+$		45760		2.00		790	0.70
$2^5\Sigma^-$		46200		1.83		600	
$3^5\Sigma^-$		48575		1.79		1040	

[a] Ref. [13].
[b] Ref. [14].
[c] Ref. [16].
[d] Ref. [17].
[e] Ref. [18].
[f] Ref. [15].
[g] Ref. [23].
[h] Ref. [9].
[i] Ref. [11].
[j] Ref. [16].
[k] Ref. [5].

that of the ground state. The computed vibrational frequency (ω_e) of the state is 975 cm^{-1}. In general, the spectroscopic parameters of the $a^1\Sigma^+$ state computed here agree well with the set of data obtained from other calculations [11]. There exists a close-lying $b^1\Pi$ state with an estimated T_e of 6725 cm^{-1} which is somewhat smaller than the value predicted from the HF+SD calculation. The equilibrium bond length as well as the vibrational frequency of $b^1\Pi$ are comparable with those of its triplet counterpart, namely the ground state. As expected, the leading configuration characterizing the $b^1\Pi$ state is the same as that of the ground state. The $\sigma_1^2\sigma_2^2\pi_1^2$ configuration not only generates the first excited state as discussed above but also two strongly bound singlets, namely $c^1\Delta$ and $d^1\Sigma^+$. The estimated transition energy of $c^1\Delta$ is 9135 cm^{-1} which is comparable with the value reported in the previous calculations

[11,16]. However, the calculation of Bruna et al. [5] predicted its transition energy above 10 500 cm^{-1}. The ω_e value of the $c^1\Delta$ state estimated here is 790 cm^{-1} which is 65 cm^{-1} smaller than the value reported in earlier calculations. The $d^1\Sigma^+$ state is the second root of the $^1\Sigma^+$ symmetry. At the equilibrium bond length, the state is dominated by an open shell configuration, $\sigma_1^2\sigma_2^2\pi_1^2$(60%), while there is at least 17% contribution of a closed shell configuration, $\sigma_1^2\pi_1^4$. The computed transition energy of this state ($T_e = 12\ 705\ cm^{-1}$) agrees well, while the r_e value reported here is 0.05 Å longer than the value reported earlier [11]. The vibrational frequency of $d^1\Sigma^+$ at r_e is about 880 cm^{-1} which is 100 cm^{-1} smaller than the value estimated in the earlier study [15].

There is a low-lying $^5\Pi$ state which has not been identified before. The state originates from a $\sigma_1^2\sigma_2\pi_1^2\pi_2$(82%) configuration in which π_2 is mostly antibonding MO comprising the $p_{x/y}$ orbitals of both Si and C. The computed transition energy of the state is about 14 460 cm^{-1} with $\omega_e = 635\ cm^{-1}$ and $r_e = 1.97$ Å. The state is also strongly bound with an estimated binding energy of 2.22 eV. Although $^5\Pi$ is not a very important state from the spectroscopic point of view, its spin components with $\Omega = 0^+$, 0^-, 1, 2, and 3 may influence the lower states to some extent. Several other excited quintet bound states of the SiC radical lie above 30 000 cm^{-1}.

The next two important states of SiC are $B^3\Sigma^+$ and $C^3\Pi$. The B state is the lowest root of the $^3\Sigma^+$ symmetry. Ab initio based CASSCF-CCI calculations of Larsson [9] have predicted the $B^3\Sigma^+$ state to lie around 18 954 cm^{-1} with a bond length of 1.67 Å. In the present calculation, the estimated T_e of this state is about 19 800 cm^{-1}. The computed bond length is 0.01 Å longer, while the calculated vibrational frequency of this state agrees well with the value reported in the earlier calculation of Larsson [9]. However, spectroscopic constants of the $B^3\Sigma^+$ state obtained from both the theoretical calculations disagree with those derived from the absorption spectrum of the $B^3\Sigma^+ \leftarrow X^3\Pi$ transition in a 5 K neon matrix. The origin of the observed band has been reported to be at 11 749 cm^{-1}. The observed ω_e of 1178 cm^{-1} also disagrees completely with the present value of 890 cm^{-1}. The spectrum of the $B^3\Sigma^+$–$X^3\Pi$ transition of SiC may need further experimental study. However, it is quite clear that there is no other lower state except the ground one to which the transition from $B^3\Sigma^+$ may take place. Theoretically, the B–X transition is expected to carry a reasonably large intensity. Around the potential minimum, the $B^3\Sigma^+$ state is characterized by two important configurations, $\sigma_1\sigma_2\pi_1^4$(45%) and $\sigma_1^2\pi_1^3\pi_2$(30%).

The $C^3\Pi$ state is the second root of the ground-state symmetry and it originates predominantly from the same configuration, $\sigma_1^2\sigma_2\pi_1^2\pi_2$ that generates the lowest $^5\Pi$. This configuration also generates eight more states of Π and Φ symmetries. The transition energy (T_e) of $C^3\Pi$ calculated here is about 21 915 cm^{-1} which is somewhat smaller than the observed value of 22 830.4(9) cm^{-1} determined from the $C^3\Pi$–$X^3\Pi$ band system of the SiC radical produced by laser vaporization. In another experimental study [18], analyses of seven rovibronic bands involving the $C^3\Pi(v' = 0–6)$–$X^3\Pi(v'' = 0)$ transition have resulted T_e and ω_e values of 22 829.46 and 615.85 cm^{-1}, respectively. The Si–C bond in the $C^3\Pi$ state is nearly 0.21 Å longer than that in the ground state. However, the calculated r_e is 0.03 Å longer than the experimentally determined value of 1.919 Å. The fitted vibrational frequency is about 580 cm^{-1}, as compared to the observed value of 615.7(8) cm^{-1}. The molecular constants computed by Larsson [9] are in better agreement with the observed data as shown in Table 1.

No other state beyond $C^3\Pi$ has been identified so far. We have predicted $^1\Sigma^-$ and $^3\Delta$ states with their potential minima located almost at the same bond length of 2.18 Å. The estimated transition energies of $^1\Sigma^-$ and $^3\Delta$ states are 23 245 and 24 485 cm^{-1}, respectively. Potential energy curves of these states are bit shallow compared to those of the other low-lying states already discussed. This has been reflected in their smaller ω_e values. Both the states originate from the same configuration, $\sigma_1^2\sigma_2^2\pi_1\pi_2$ with the same dominance at equilibrium. We may therefore, expect a $^3\Delta$–$X^3\Pi$ transition to take place around 24 500 cm^{-1}. Although such a transition has not yet been observed, we have labelled $^3\Delta$ as the D state because it is next to $C^3\Pi$. There is another excited $^3\Pi$, denoted as $E^3\Pi$ which lies just above $D^3\Delta$. The computed transition energy of the $E^3\Pi$ state is about 25 875 cm^{-1}. The state originates from $\sigma_1^2\sigma_2\pi_1^2\pi_2$(78%) which has also created the lower lying $C^3\Pi$ and $^5\Pi$ states. The r_e and ω_e values of the $E^3\Pi$ state are very similar to those of $C^3\Pi$. The $E^3\Pi$ state, however, dissociates into the higher asymptote. The E–X transition is expected to be strong one though no such transition is experimental reported so far.

The second root of $^1\Pi$, which is also characterized by the $\sigma_1^2\sigma_2\pi_1^2\pi_2$ configuration, is weakly bound. The potential minimum of the $2^1\Pi$ state is located around the bond length of 2.02 Å with an estimated transition energy of 27 415 cm^{-1} at equilibrium. Both the lowest singlet and triplet Φ states are strongly bound and have similar spectroscopic properties. The energy separation between them is about 5300 cm^{-1} with the $^3\Phi$ state lying lower. These states are also predominantly characterized by the same configuration that generates $^5\Pi$, $C^3\Pi$, $E^3\Pi$, and $2^1\Pi$. The $^3\Phi$–$X^3\Pi$ transition may be of some interest from the spectroscopic point of view.

Potential energy curves of three lowest states of the $^3\Sigma^+$ symmetry undergo avoided crossings as seen in Fig. 1a. Analyzing the compositions of these states in the CI calculations, it has been found that three important configurations, namely $\sigma_1\sigma_2\pi_1^4$, $\sigma_1^2\pi_1^3\pi_2$, and $\sigma_1^2\sigma_2^2\pi_1\pi_2$ mix up. An avoided curve crossing between the first and second root of $^3\Sigma^+$ takes place around $3.9a_0$, while another crossing is noted between the second and third root in the range $3.2–3.4a_0$. The contributions of important configurations of all three $^3\Sigma^+$ states over a certain range of bond distances have been displayed in Table 2.

Table 2
Compositions (% contribution) of the lowest three roots of $^3\Sigma^+$ of SiC in the bond length range 2.7–4.2 bohr

r/bohr	$B^3\Sigma^+$	$2^3\Sigma^+$	$3^3\Sigma^+$
2.7	$\sigma_1\sigma_2\pi_1^4(70)$, $\sigma_1^2\pi_1^3\pi_2(8)$	$\sigma_1^2\pi_1^3\pi_2(69)$ $\sigma_2^2\pi_1^3\pi_2(4)$, $\sigma_1\sigma_2\pi_1^4(9)$,	$\sigma_1\sigma_2\pi_1^3\pi_2(80)$, $\sigma_1\sigma_2\pi_1^4(6)$
2.9	$\sigma_1\sigma_2\pi_1^4(63)$, $\sigma_1^2\pi_1^3\pi_2(13)$, $\sigma_1\sigma_2\pi_1^3\pi_2(6)$	$\sigma_1^2\pi_1^3\pi_2(64)$, $\sigma_1\sigma_2\pi_1^4(14)$	$\sigma_1^2\sigma_2^2\pi_1\pi_2(82)$
3.1	$\sigma_1\sigma_2\pi_1^4(52)$, $\sigma_1^2\pi_1^3\pi_2(22)$, $\sigma_1\sigma_2\pi_1^3\pi_2(6)$	$\sigma_1^2\pi_1^3\pi_2(54)$, $\sigma_1\sigma_2\pi_1^4(23)$	$\sigma_1^2\sigma_2^2\pi_1\pi_2(82)$
3.2	$\sigma_1\sigma_2\pi_1^4(45)$, $\sigma_1^2\pi_1^3\pi_2(29)$, $\sigma_1\sigma_2\pi_1^3\pi_2(4)$	$\sigma_1^2\pi_1^3\pi_2(45)$, $\sigma_1\sigma_2\pi_1^4(27)$	$\sigma_1^2\sigma_2^2\pi_1\pi_2(80)$, $\sigma_1^2\pi_1^3\pi_2(4)$
3.5	$\sigma_1^2\pi_1^3\pi_2(53)$, $\sigma_1\sigma_2\pi_1^4(20)$	$\sigma_1^2\sigma_2^2\pi_1\pi_2(80)$	$\sigma_1\sigma_2\pi_1^4(45)$, $\sigma_1^2\pi_1^3\pi_2(25)$
3.6	$\sigma_1^2\pi_1^3\pi_2(57)$, $\sigma_1\sigma_2\pi_1^4(13)$	$\sigma_1^2\sigma_2^2\pi_1\pi_2(80)$	$\sigma_1\sigma_2\pi_1^4(51)$, $\sigma_1^2\pi_1^3\pi_2(19)$
3.8	$\sigma_1^2\pi_1^3\pi_2(49)$, $\sigma_1^2\sigma_2^2\pi_1\pi_2(27)$	$\sigma_1^2\sigma_2^2\pi_1\pi_2(60)$, $\sigma_1^2\pi_1^3\pi_2(17)$	$\sigma_1\sigma_2\pi_1^4(54)$, $\sigma_1^2\pi_1^3\pi_2(11)$
3.9	$\sigma_1^2\sigma_2^2\pi_1\pi_2(55)$, $\sigma_1^2\pi_1^3\pi_2(26)$	$\sigma_1^2\pi_1^3\pi_2(41)$, $\sigma_1^2\sigma_2^2\pi_1\pi_2(30)$	$\sigma_1\sigma_2\pi_1^4(53)$, $\sigma_1^2\pi_1^3\pi_2(8)$, $\sigma_1\sigma_2\pi_1^3\pi_2(8)$
4.2	$\sigma_1^2\sigma_2^2\pi_1\pi_2(74)$, $\sigma_1^2\pi_1^3\pi_2(11)$	$\sigma_1^2\pi_1^3\pi_2(59)$, $\sigma_1^2\sigma_2^2\pi_1\pi_2(11)$	$\sigma_1\sigma_2\pi_1^4(38)$, $\sigma_1\sigma_2\pi_1^3\pi_2(12)$, $\sigma_1^2\sigma_2\sigma_6\pi_1^2(7)$, $\sigma_1\sigma_2\pi_1^2\pi_2^2(5)$

Two excited $^3\Sigma^-$ states, namely $2^3\Sigma^-$ and $3^3\Sigma^-$ also undergo an avoided crossing around the bond length of $3.6a_0$. This is reflected in the potential energy curves of these states shown in Fig. 1a. The diabatic coupling is considerably large. In the bond length region below $3.6a_0$, the lower root is dominated by $\sigma_1^2\pi_1^3\pi_2$, while in the other region it is mainly characterized by the $\sigma_1^2\sigma_2^2\pi_1\pi_2$ configuration. The diabatic curve of the $2^3\Sigma^-$ state is predicted to have a minimum around 2.2 Å with an estimated transition energy of 33 100 cm^{-1}. We also expect the diabatic curve of $3^3\Sigma^-$ to have a potential minimum around 1.8 Å with a predicted transition energy of about 36 200 cm^{-1}.

Both the $^5\Sigma^+$ states reported here are weakly bound and dissociate into the lowest limit through different channel. The potential minimum of $^5\Sigma^+$ is located at 1.78 Å with $\omega_e = 745$ cm^{-1} and $T_e = 33\ 355$ cm^{-1}. Around the equilibrium bond length, the $^5\Sigma^+$ state is characterized predominantly by $\sigma_1\sigma_2\pi_1^3\pi_2$, while another configuration, $\sigma_1^2\pi_1^2\pi_2^2$ dominates at the longer bond distances. This has resulted a predissociation of the $^5\Sigma^+$ state through a barrier of height 0.22 eV. A strong avoided crossing between the potential curves of the two roots of $^5\Sigma^+$ has created an apparent minimum in the potential curve of $2^5\Sigma^+$. Since the coupling between these two roots is very strong, we have fitted the adiabatic curve and the minimum is located at 2.0 Å with $\omega_e = 790$ cm^{-1} and $T_e = 45\,735$ cm^{-1}. The nature of the potential energy curve of $2^5\Sigma^+$ reveals that there is a potential barrier of height 0.4 eV at 4.4 a_0 beyond which the state dissociates through a repulsive path.

Three more excited singlets, namely $3^1\Sigma^+$, $2^1\Sigma^-$, and $2^1\Delta$ of the SiC radical are strongly bound. They correlate with the higher asymptote, $Si(^1D_g)+C(^1D_g)$. The predicted transition energy of the $3^1\Sigma^+$ state is about 35 125 cm^{-1} at $r_e = 1.72$ Å. The estimated vibrational frequency of the state is close to that of $a^1\Sigma^+$. A transition of the type $3^1\Sigma^+ - a^1\Sigma^+$ is expected to occur around 29 000 cm^{-1} with a large transition probability. Both $2^1\Sigma^-$ and $2^1\Delta$ states in the Franck–Condon region are characterized mainly by the $\sigma_1^2\pi_1^3\pi_2$ configuration. The potential energy curve of $2^1\Delta$ shows an avoided crossing near the bond distance of $4.0a_0$. The estimated r_es of $2^1\Sigma^-$ and $2^1\Delta$ are 1.84 and 1.82 Å, respectively. Analyzing the compositions of these states above $4.0a_0$, a strong mixing with other configurations is predicted. The vibrational frequency of the $2^1\Delta$ state is nearly 100 cm^{-1} smaller than that of $2^1\Sigma^-$. The computed transition energies of these two excited singlets lie in the range 37 000–39 000 cm^{-1}.

The lowest $^5\Delta$ state has a deep potential minimum at $r_e = 1.73$ Å with $T_e = 42\,005$ cm^{-1} and it is mainly described by the $\sigma_1\sigma_2\pi_1^3\pi_2(82\%)$ configuration. Potential energy curves in Fig. 1c show that there is an avoided crossing around $4.1a_0$ with a repulsive curve of an excited $^5\Delta$ which is dominated by the $\sigma_1^2\sigma_2\sigma_6\pi_1\pi_2$ configuration. This has resulted a predissociation of $^5\Delta$ to the lowest dissociation limit through a large barrier of 1.3 eV. However, the fitted potential curve in the Franck–Condon region has predicted $\omega_e = 963$ cm^{-1}. The second and third root of $^5\Sigma^-$ have bound potential energy curves. The compositions of these roots at different bond distances reveal that there is a strong mixing between $(\sigma_1\sigma_2\pi_1^3\pi_2)^5\Sigma^-$ and $(\sigma_1^2\sigma_2\sigma_3\pi_1^2)^5\Sigma^-$ in the range 3.4–3.5a_0. As a result, the potential minimum of $2^5\Sigma^-$ is shallow, while the adiabatic curve of $3^5\Sigma^-$ is very sharp with a large ω_e of 1040 cm^{-1}. The estimated r_e of the $3^5\Sigma^-$ state is about 1.79 Å, while the minimum of the adiabatic curve of $2^5\Sigma^-$ is located around the bond length of 1.83 Å with $\omega_e = 600$ cm^{-1}.

In Table 1, we have reported the computed dipole moments (μ_e) of most of the low-lying states at their equilibrium bond lengths. The ground-state μ_e is estimated to be about 1.62 D with Si^+C^- polarity. The first excited state ($A^3\Sigma^-$) has a larger μ_e value of 2.55 D. All other excited states have the same sense of polarity as that of the ground state.

3.2. Spectroscopic constants and potential energy curves of Ω states

The spin–orbit coupling splits the ground-state dissociation limit, $Si(^3P_g)+C(^3P_g)$ into nine very closely spaced asymptotes. The largest splitting is only 267 cm^{-1} as obtained from the observed atomic spectral data [38]. These asymptotes correlate with 50 Ω states of the SiC radical. In the present calculations, we allow all these states to interact. Potential energy curves of a few low-lying states of 0^+, 0^-, 1, and 2 symmetries of SiC are shown in Fig. 2a–d. Since both the atoms are light, the spin–orbit effects are expectedly small. The potential energy curves show no great changes and the avoided crossings are very sharp.

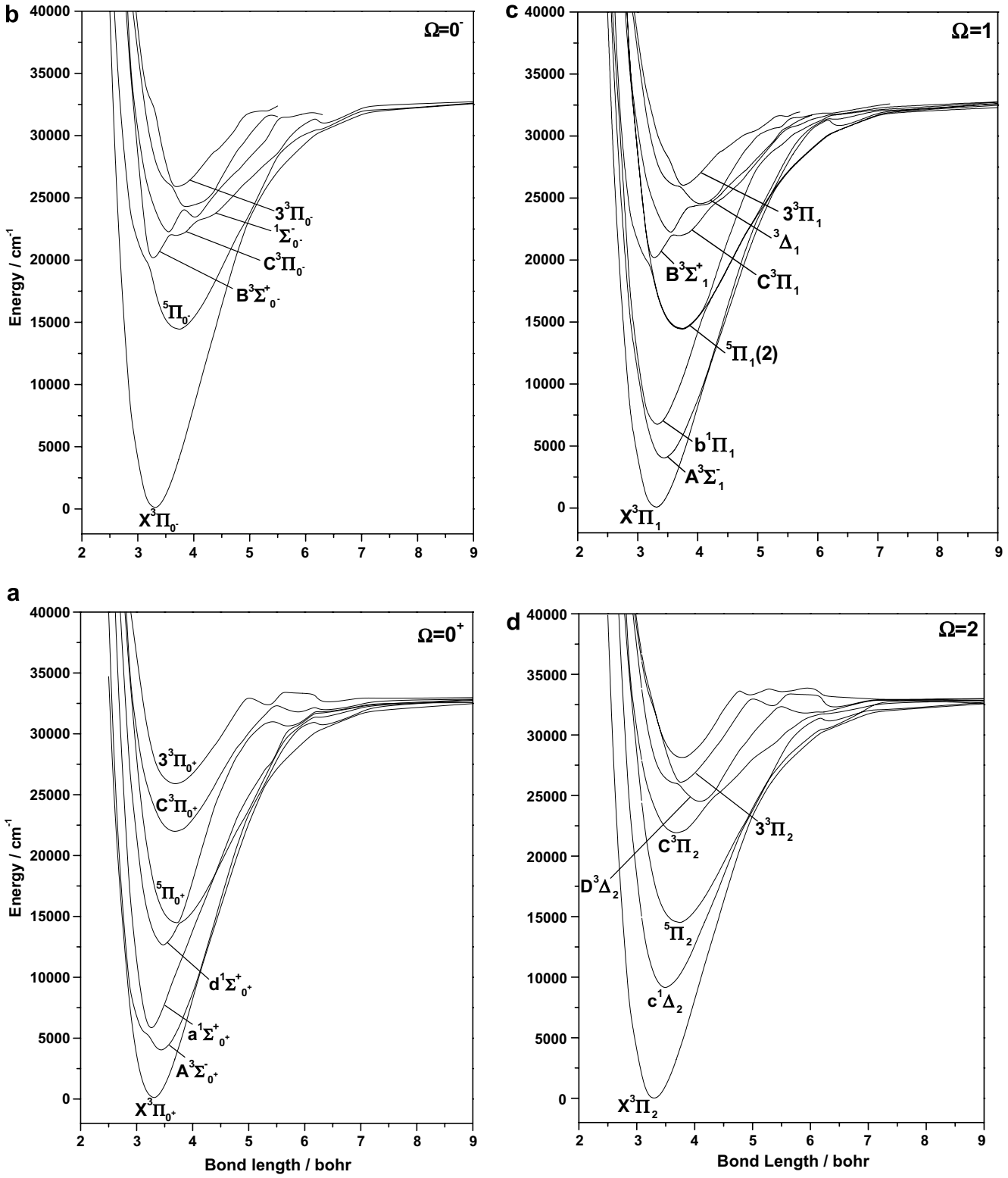

Fig. 2. Computed potential energy curves of a few low-lying Ω states of the SiC radical: (a) $\Omega = 0^+$, (b) $\Omega = 0^-$, (c) $\Omega = 1$, and (d) $\Omega = 2$.

The ground state of SiC splits in an inverted order with $X^3\Pi_2$ being the lowest spin–orbit component. All four components of $X^3\Pi$ lie within 100 cm^{-1}. The computed spectroscopic constants of the low-lying Ω states up to 22 000 cm^{-1} of energy are shown in Table 3. The spin–orbit mixing does not change the spectroscopic constants much. The two components of $A^3\Sigma^-$ are almost inseparable. The transition energies are increased only by 70–75 cm^{-1} due to the spin–orbit coupling. All the singlet components, $a^1\Sigma^+_{0^+}$, $b^1\Pi_1$, $c^1\Delta_2$, and $d^1\Sigma^+_{0^+}$ remain almost unchanged in their

Table 3
Spectroscopic constants of low-lying Ω states of SiC

State	T_e/cm^{-1}	r_e/Å	ω_e/cm^{-1}
$X^3\Pi_2$	0 (0)[a]	1.74	930
$X^3\Pi_1$	60 (37.3)[a]	1.74	925
$X^3\Pi_{0^-}$	95 (74.6)[a]	1.74	933
$X^3\Pi_{0^+}$	100 (74.6)[a]	1.74	933
$A^3\Sigma_1^-$	4055	1.82	854
$A^3\Sigma_{0^+}^-$	4060	1.82	855
$a^1\Sigma_{0^+}^+$	5370	1.68	975
$b^1\Pi_1$	6770	1.76	931
$c^1\Delta_2$	9185	1.85	800
$d^1\Sigma_{0^+}^+$	12745	1.84	882
$^5\Pi_1$	14450	1.97	625
$^5\Pi_{0^-}$	14480	1.97	625
$^5\Pi_{0^+}$	14485	1.97	625
$^5\Pi_1$	14515	1.97	625
$^5\Pi_2$	14550	1.97	625
$^5\Pi_3$	14585	1.97	625
$B^3\Sigma_1^+$	19880	1.69	871
$B^3\Sigma_{0^-}^+$	19885	1.69	871
$C^3\Pi_2$	21935	1.95	581
$C^3\Pi_1$	21965	1.95	581
$C^3\Pi_{0^-}$	21995	1.95	581
$C^3\Pi_{0^+}$	22000	1.95	582

[a] Ref. [16].

spectroscopic properties. The spin–orbit components of $^5\Pi$ split in a regular order with a maximum separation of 135 cm^{-1}. The components of $C^3\Pi$, however, split in an inverted order as displayed in Table 3. Spectroscopic properties of the 0^- and 1 components of $B^3\Sigma^+$ are nearly the same.

3.3. Transition properties

Several electric dipole allowed transitions involving the low-lying singlets and triplets of SiC are studied here. Transition probabilities of six triplet–triplet transitions, each of which has the ground state as the lowest one, have been computed. Transition dipole moments of these transitions as a function of bond distance are shown in Fig. 3a. The transition-moment curve of $A^3\Sigma^-$–$X^3\Pi$ is smoothly decreasing to zero at the longer bond distance. In the Franck–Condon region, the magnitude of the transition dipole moment of A–X is about $0.3ea_0$. The computed partial radiative lifetime for this transition at $v' = 0$ is about 125 μs and it decreases considerably with the higher v'. Table 4 lists the partial radiative lifetimes for eleven transitions at the lowest three vibrational levels. The $B^3\Sigma^+$–$X^3\Pi$ transition moments in the Franck–Condon region are at least 10 times smaller than those of A–X. But the computed lifetime for the B–X transition is lower due to larger energy differences. As expected, transitions from the excited Π states to the ground state are relatively strong. Transition moment curves for both $C^3\Pi$–$X^3\Pi$ and $E^3\Pi$–$X^3\Pi$ look similar (Fig. 3a). These two transitions are predicted to be more probable than either the A–X or B–X transition. The radiative lifetime for the $C^3\Pi$–$X^3\Pi$ transition at the

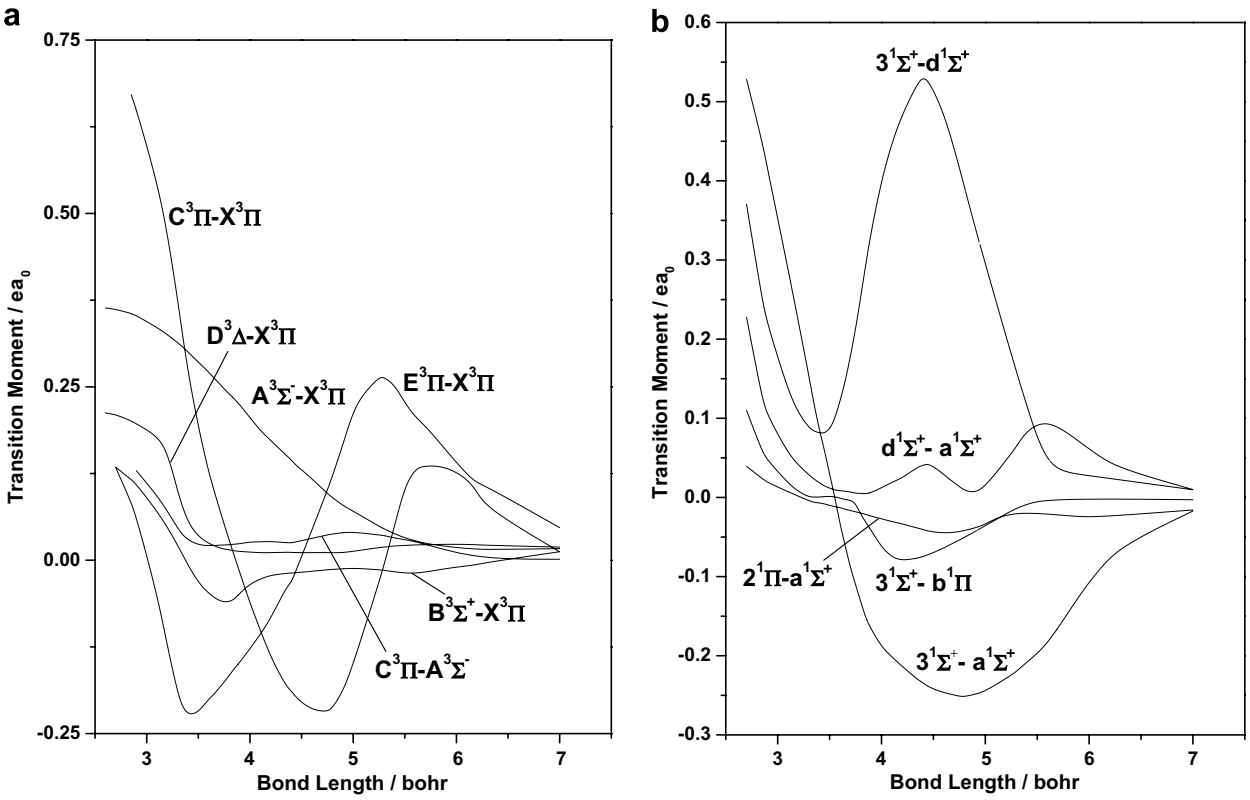

Fig. 3. Transition dipole moment functions of low-lying Λ–S states of the SiC radical: (a) triplets and (b) singlets.

Table 4
Radiative lifetimes (μs) of some excited states of SiC

Transition	Lifetimes of the upper state		
	$v' = 0$	$v' = 1$	$v' = 2$
$A^3\Sigma^-$–$X^3\Pi$	125 (107.6)[a]	105 (82.3)[a]	91 (67.0)[a]
$B^3\Sigma^+$–$X^3\Pi$	28.7	28.9	26.3
$C^3\Pi$–$X^3\Pi$	5.15	2.78	1.88
$C^3\Pi$–$A^3\Sigma^-$	216	188	156
$D^3\Delta$–$X^3\Pi$	1250	970	760
$E^3\Pi$–$X^3\Pi$	1.10	1.17	1.25
$3^1\Sigma^+$–$a^1\Sigma^+$	0.51	0.47	0.43
$3^1\Sigma^+$–$b^1\Pi$	485	195	128
$3^1\Sigma^+$–$d^1\Sigma^+$	5.58	5.06	4.34
$d^1\Sigma^+$–$a^1\Sigma^+$	9110	3800	2100
$2^1\Pi$–$a^1\Sigma^+$	303	307	350

[a] Ref. [14].

lowest vibrational level is about 5.15 μs. The computed partial lifetime for another transition, $C^3\Pi$–$A^3\Sigma^-$ is 216 μs at $v' = 0$. The total radiative lifetime of the $C^3\Pi$ state, computed after adding the transition probabilities of C–X and C–A transitions is about 5.03 μs. However, this value is nearly 1.75 times longer than the experimentally determined [18] value of 2.886 μs. The transition probability of another possible transition, $C^3\Pi$–$B^3\Sigma^+$ is very low as the energy difference is only about 2000 cm^{-1}. The $E^3\Pi$–$X^3\Pi$ transition is found to be the strongest of all triplet–triplet transitions and it is expected to appear in the range 25 000–26 000 cm^{-1}. The computed radiative lifetime for this transition is estimated to be 1.1 μs in the lowest vibrational level.

Transition probabilities of five singlet–singlet transitions are computed. The transition dipole moment functions of these transitions are shown in Fig. 3b. Three transitions from the $3^1\Sigma^+$ state, namely $3^1\Sigma^+$– $a^1\Sigma^+$, $3^1\Sigma^+$–$B^1\Pi$, and $3^1\Sigma^+$– $d^1\Sigma^+$ are studied. The $3^1\Sigma^+$– $a^1\Sigma^+$ transition has the largest transition probability. The computed radiative lifetime for this transition is about 510 ns at $v' = 0$. Adding the transition probabilities of these three transitions, the total radiative lifetime of the $3^1\Sigma^+$ state is estimated to be 467 ns at the lowest vibrational level. However, no transition from the $3^1\Sigma^+$ state of SiC is experimentally known yet. Among the other transitions reported here, the $2^1\Pi$–$a^1\Sigma^+$ transition is predicted to be stronger than $d^1\Sigma^+$–$a^1\Sigma^+$. The computed lifetime of the former transition is about 300 μs.

4. Summary

Low-lying electronic states of the SiC radical have been studied by using ab initio based MRDCI calculations which include pseudo potentials of both Si and C atoms. We have compared the computed spectroscopic constants with the observed and previously calculated data. At least 23 states of Λ–S symmetries have been reported within 6 eV of energy. Besides the ground state, the triplets such as $A^3\Sigma^-$, $B^3\Sigma^+$, and $C^3\Pi$ are experimentally well studied. Four singlets, $a^1\Sigma^+$, $b^1\Pi$, $c^1\Delta$, and $d^1\Delta$ are located in between 5000 and 13 000 cm^{-1}. The lowest bound state of the quintet spin multiplicity is $^5\Pi$ which is located around 14 460 cm^{-1}. Potential energy curves of all the low-lying states are constructed. The excited $E^3\Pi$ state is not previously known. We have predicted that the transition energy of the $E^3\Pi$ state is about 25 875 cm^{-1}. Its r_e and ω_e are 1.94 Å and 600 cm^{-1}, respectively. A number of singlet and quintet states exist in between 30 000 and 50 000 cm^{-1}. Some of these singlet and quintet states are strongly bound. The ground-state dipole moment (μ_e) is calculated to be 1.62 D with a Si^+C^- polarity. All the other excited states have the same sense of polarity. The largest dipole moment is reported for the $A^3\Sigma^-$ state. The spin–orbit effects on the low-lying states of SiC are not significant to change their spectroscopic properties. The largest splitting among the four spin components of $X^3\Pi$ is only 100 cm^{-1} with $X^3\Pi_2$ being the lowest one. The two components of both $A^3\Sigma^-$ and $B^3\Sigma^+$ are inseparable. Several electric dipole allowed triplet–triplet and singlet–singlet transitions at the Λ–S level have been studied. The strongest triplet–triplet transition is predicted to be $E^3\Pi$–$X^3\Pi$ in the range 25 000–26 000 cm^{-1}. The computed radiative lifetime of this transition at $v' = 0$ is 1.1 μs. However, such a transition has not been observed yet. The computed radiative lifetime of $C^3\Pi$ is 5.03 μs compared to the experimentally determined value of 2.886 μs. The lifetimes for A–X and B–X transitions are predicted to be 125 and 28.7 μs, respectively. Of three transitions from the excited $3^1\Sigma^+$ state, the $3^1\Sigma^+$–$a^1\Sigma^+$ transition has the largest transition probability and it has the shortest lifetime ($\tau = 510$ ns at $v' = 0$) among all the transitions studied here.

Acknowledgments

K.K.D. thanks UGC, Govt. of India for the financial support under the Major Research Project. A.P. also thanks CSIR, Govt. of India for the award of a Junior Research Fellowship. The authors thank Prof. R.J. Buenker, Wuppertal, Germany for providing the CI codes.

References

[1] A. Suzuki, Prog. Theor. Phys. 62 (1979) 936.
[2] V.E. Bondybey, J. Phys. Chem. 86 (1982) 3396.
[3] D.L. Michalopoulos, M.E. Geusic, P.R.R. Langridge-Smith, R.E. Smalley, J. Chem. Phys. 80 (1984) 3556.
[4] B.L. Lutz, J.A. Ryan, Astrophys. J. 194 (1974) 753.
[5] P.J. Bruna, S.D. Peyerimhoff, R.J. Buenker, J. Chem. Phys. 72 (1980) 5437.
[6] C.M. Rohlfing, R.L. Martin, J. Phys. Chem. 90 (1986) 2043.
[7] J. Anglada, P.J. Bruna, S.D. Peyerimhoff, R.J. Buenker, Mol. Phys. 16 (1983) 2469.
[8] H. Dohman, P.J. Bruna, S.D. Peyerimhoff, R.J. Buenker, Mol. Phys. 51 (1984) 1109.
[9] M. Larsson, J. Phys. B: At. Mol. Phys. 19 (1986) L261.
[10] C. Bauschlicher Jr., S.R. Langhoff, J. Chem. Phys. 87 (1987) 2919.
[11] P.F. Bernath, S.A. Rogers, L.C. O'Brien, C.R. Brazier, Phys. Rev. Lett. 60 (1988) 197.

[12] J. Cernicharo, C.A. Gottlieb, M. Guelin, P. Thaddeus, J.M. Vrtilek, Astrophys. J. Lett. 341 (1989) L25.
[13] C.R. Brazier, L.C. O′Brien, P.F. Bernath, J. Chem. Phys. 91 (1989) 7384.
[14] S.R. Langhoff, C. Bauschlicher Jr., J. Chem. Phys. 93 (1990) 42.
[15] F.L. Sefyani, J. Schamps, Astrophys. J. 434 (1994) 816.
[16] J.M.L. Martin, J.P. Francois, R. Gijbels, J. Chem. Phys. 92 (1990) 6655.
[17] T.J. Butenhoff, E.A. Rohlfing, J. Chem. Phys. 95 (1991) 3939.
[18] M. Ebben, M. Drabbels, J.J. ter Meulen, J. Chem. Phys. 45 (1991) 2292.
[19] A.D. McLean, B. Liu, G.S. Chandler, J. Chem. Phys. 97 (1992) 8459.
[20] R. Mollaaghababa, C.A. Gottlieb, J.M. Vrtilek, P. Thaddens, Astrophys. J. Lett. 352 (1990) L21.
[21] R. Mollaaghababa, C.A. Gottlieb, J.M. Vrtilek, P. Thaddens, J. Chem. Phys. 98 (1993) 968.
[22] A.I. Boldyrev, J. Simons, V.G. Zahrzewski, W. Von Niessen, J. Phys. Chem. 98 (1994) 1427.
[23] M. Grutter, P. Freivogel, J.P. Mair, J. Phys. Chem. A 101 (1997) 275.
[24] M.N. Deo, K.J. Kawaguchi, Mol. Spectrosc. 228 (2004) 76.
[25] L.F. Pacios, P.A. Christiansen, J. Chem. Phys. 82 (1985) 2664.
[26] J.M.O. Matos, V. Kellö, B.O. Ross, A.J. Sadlej, J. Chem. Phys. 89 (1988) 423.
[27] R.J. Buenker, S.D. Peyerimhoff, Theo. Chim. Acta 35 (1974) 33.
[28] R.J. Buenker, S.D. Peyerimhoff, Theo. Chim. Acta 39 (1975) 217.
[29] R.J. Buenker, Int. J. Quantum Chem. 29 (1986) 435.
[30] R.J. Buenker, in: P. Burton (Ed.), Proceedings of Workshop on Quantum Chemistry and Molecular Physics in Wollongong, Wollongong, Australia, 1980.
[31] R.J. Buenker, in: R. Carbò (Ed.), Studies in physical and theoretical chemistry, Current Aspects of Quantum Chemistry, vol. 21, Elsevier, Amsterdam, 1982, p. 17.
[32] R.J. Buenker, S.D. Peyerimhoff, W. Butscher, Mol. Phys. 35 (1978) 771.
[33] R.J. Buenker, R.A. Philips, J. Mol. Struct. (Theochem) 123 (1985) 291.
[34] S. Krebs, R.J. Buenker, J. Chem. Phys. 103 (1995) 5613.
[35] E.R. Davidson, in: R. Daudel, B. Pullman (Eds.), The World of Quantum Chemistry, Reidel Dordrecht, The Netherland, 1974.
[36] G. Hirsch, P.J. Bruna, S.D. Peyerimhoff, R.J. Buenker, Chem. Phys. Lett. 52 (1977) 442.
[37] A.B. Alekseyev, R.J. Buenker, H.-P. Lieberman, G. Hirsch, J. Chem. Phys. 100 (1994) 2989.
[38] C.E. Moore, Tables of Atomic Energy Levels, vols. I–III, U.S. National Bureau of Standards, Washington, DC, 1971.
[39] J. Drowart, G. De Maria, M.G. Inghram, J. Chem. Phys. 29 (1958) 1015.
[40] G. Verhaegen, F.E. Stafford, J. Drowart, J. Chem. Phys. 40 (1964) 1622.
[41] P.J. Bruna, C. Petrongolo, R.J. Buenker, S.D. Peyerimhoff, J. Chem. Phys. 74 (1981) 4611.